

# VLR-Driver: Large Vision-Language-Reasoning Models for Embodied Autonomous Driving

Anonymous ICCV submission

Paper ID 14508

## Abstract

The rise of embodied intelligence and multi-modal large language models has led to exciting advancements in the field of autonomous driving, establishing it as a prominent research focus in both academia and industry. However, when confronted with intricate and ambiguous traffic scenarios, the lack of logical reasoning and cognitive decision-making capabilities remains the primary challenge impeding the realization of embodied autonomous driving. Although Vision Language Models (VLMs) have enhanced the deep semantic understanding of autonomous driving systems, they exhibit notable limitations in decision explainability when handling rare and long-tail traffic scenarios. In this paper, we propose VLR-Driver, a novel multi-modal Vision-Language-Reasoning (VLR) framework based on Chain of Thought (CoT) for embodied autonomous driving. The framework employs a spatiotemporal CoT reasoning approach to recursively analyze potential safety risks and driving intentions of other agents, thereby delivering an efficient and transparent decision-making process. Furthermore, we construct a multi-modal reasoning-decision dataset to support the advancement of hierarchical reasoning of VLMs in autonomous driving. Closed-loop experiments conducted in CARLA demonstrate that the VLR-Driver significantly outperforms state-of-the-art end-to-end methods. Notably, key metrics such as driving score improved by 17.5%, while the success rate improved by 22.2%, offering a more transparent, reliable, and secure solution for autonomous driving systems. The code, dataset, and demonstration video will be open-sourced.

## 1. Introduction

In recent years, the rapid progress of End-to-End (E2E) architectures [6, 7, 18, 49], Large Language Models (LLMs) [12, 41, 48], and embodied intelligence [26, 53, 55] has established these technologies as key enablers of innovation in autonomous driving. Especially, VLMs enriched with ex-

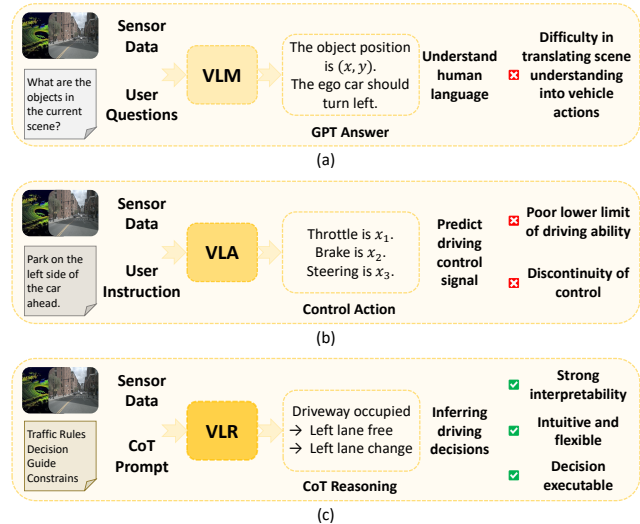


Figure 1. Comparison of different VLM-based AD systems. (a) VLM model focuses more on answering questions, but it is difficult to convert decisions into coherent control signals. (b) VLA model focuses more on predicting driving control signals, but lacks interpretability. (c) The VLR model generates decisions and controls signals with transparent reasoning processes through CoT, enhancing the driver trust in the system.

tensive pre-training knowledge exhibit strong spatial understanding and common-sense reasoning abilities. DriveVLM [35] leverages VLM to enhance spatial awareness and planning capabilities in complex driving scenarios. CoVLA [2] integrates visual perception, language understanding, and action planning, demonstrating remarkable effectiveness in describing traffic scenarios and generating executable control actions.

However, the decision-making process of VLMs often functions as a “black box”, making it challenging to trace and interpret their underlying logic. This makes it difficult for autonomous driving systems to be fully trusted by drivers when encountering complex and emergency situations, such as illegal roadside parking, navigating intersec-

036  
037  
038  
039  
040  
041  
042  
043  
044  
045  
046  
047  
048  
049

050 tions without traffic signals, and managing complex mixed-  
051 traffic interactions between motorized and non-motorized  
052 vehicles, thereby limiting their reliability and safety in real-  
053 world applications [39, 46, 54]. Moreover, most VLMs  
054 are trained on internet data, lacking spatial understanding  
055 and specialized training in the field of autonomous driving,  
056 making it difficult for them to fully adapt to dynamic and  
057 complex driving scenarios.

058 Meanwhile, CoT reasoning demonstrates strong inference-  
059 erence, interpretability, and generalization capabilities by  
060 breaking down complex tasks into intermediate reasoning  
061 steps [40]. CoT enables systems to think step by step  
062 rather than relying on E2E black-box predictions, making it  
063 one of the key approaches toward achieving embodied au-  
064 tonomous driving. Sce2DriveX [52] enhances comprehen-  
065 sive perception and reasoning by introducing a multi-modal  
066 LLM framework with CoT, enabling a deeper understand-  
067 ing of spatiotemporal relationships and road topology. Sim-  
068ilarly, DriveCoT [38] integrates CoT reasoning to improve  
069 decision-making interpretability and controllability in au-  
070 tonomous driving systems. However, existing CoT-based  
071 methods heavily depend on predefined reasoning templates  
072 or limited training data, which may lead to misguided de-  
073 cisions in complex traffic scenarios. Additionally, current  
074 method primarily operate on static snapshots rather than  
075 continuous temporal sequences, limiting their ability to pre-  
076 dict future events in dynamic traffic environments.

077 To bridge these gaps, in this work, we introduce  
078 **VLR-Driver**, a hierarchical CoT-based visual-language-  
079 reasoning model designed for closed-loop embodied au-  
080 tonomous driving. Our approach integrates the spatiotem-  
081 poral features from cross-modal data, including multi-frame  
082 multi-view images and ego-vehicle control signals, by em-  
083 ploying a SpatioTemporal CoT (ST-CoT) strategy that pro-  
084 duces human-like reflective reasoning processes and driving  
085 action decisions. Additionally, we adopt a dual-phase train-  
086 ing strategy, combining Low-Rank Adaptation (LoRA) [16]  
087 with an improved Stepwise Group Relative Policy Opti-  
088 mization (Step-GRPO) [34], significantly enhancing mem-  
089 ory capacity and deep reasoning abilities. Our proposed  
090 VLR-Driver not only inherits the global action optimization  
091 capabilities of VLA models, but also preserves the trans-  
092 parency of modular rule-based methods. When encoun-  
093 tering long-tail events and rare traffic scenarios, it demon-  
094 strates exceptional reflective reasoning and step-by-step in-  
095 ference processes, thereby enhancing human drivers’ trust  
096 in autonomous driving systems. The differences between  
097 VLM, VLA, and our proposed VLR are illustrated in Fig. 1

098 To further enhance VLR models in environmental under-  
099 standing, reasoning, and decision-making, we introduce the  
100 VLR-Driver Dataset. This data set includes detailed scene  
101 descriptions, weather information, vehicle state details, and  
102 most critically, human-like CoT reasoning processes and

103 the corresponding driving decisions. Various experiments  
104 demonstrate that VLR-Driver is capable of making accu-  
105 rate driving decisions and coherent reasoning, even under  
106 challenging and highly dynamic road conditions.

107 The primary contributions of this work are summarized  
108 as follows:

- **Distinctive VLR-Driver Framework.** We introduce  
VLR-Driver, a visual-language-reasoning model devel-  
oped for embodied autonomous driving. It generates a  
human-like reflective reasoning process within the driv-  
ing system, enabling accurate driving decisions.
- **Spatiotemporal CoT.** We present a spatiotemporal CoT  
strategy that recursively analyzes potential safety risks  
and the driving intentions of moving agents in complex  
traffic scenarios, ensuring that the reasoning process of  
driving decisions remains transparent and interpretable.
- **Advanced VLR-Driver Dataset.** We construct VLR-  
Driver Dataset, a cutting-edge visual-language-reasoning  
and decision-making dataset specifically designed for au-  
tonomous driving. It supports the enhancement of spa-  
tiotemporal understanding and reflective reasoning capa-  
bilities in embodied autonomous driving systems.
- **Superior Performance in Closed-Loop Simulations.**  
Extensive closed-loop experiments are conducted on the  
CARLA platform. On the Bench2Drive benchmark, our  
approach achieves a 17.5% improvement in driving score  
and a 22.2% increase in success rate, providing a more  
human-like, reliable, and trustworthy solution.

## 2. Related Work

### 2.1. End-to-end Autonomous Driving

The rapid advancement of E2E-AD has fostered a growing  
transition away from modular rule-based methods toward  
data-driven approaches [15, 23]. Based on different input  
modalities, E2E methods can be categorized into visual-  
only methods [5, 8, 10, 17] and vision-LiDAR fusion meth-  
ods [1, 20, 21]. TCP [42] and NEAT [10] adopt imitation  
learning methods, training directly on collected state-  
action pair datasets, demonstrating the feasibility of E2E  
approaches for autonomous driving. Roach [51] utilizes re-  
inforcement learning experts as coaches, delivering dense  
and informative supervision signals to agents equipped with  
monocular camera inputs. However, vision-based meth-  
ods inherently struggle with distance and depth estimation.  
These limitations may compromise the reliability of driving  
decisions [25]. To address these limitations, vision-LiDAR  
fusion methods such as TransFuser [11], CrossFuser [43],  
and FusionAD [47] have been designed to effectively in-  
tegrate image with LiDAR data, significantly improving  
the robustness of AD systems in complex environments.  
However, different modalities contribute differently to the  
driving task, and spatiotemporal synchronization issues be-

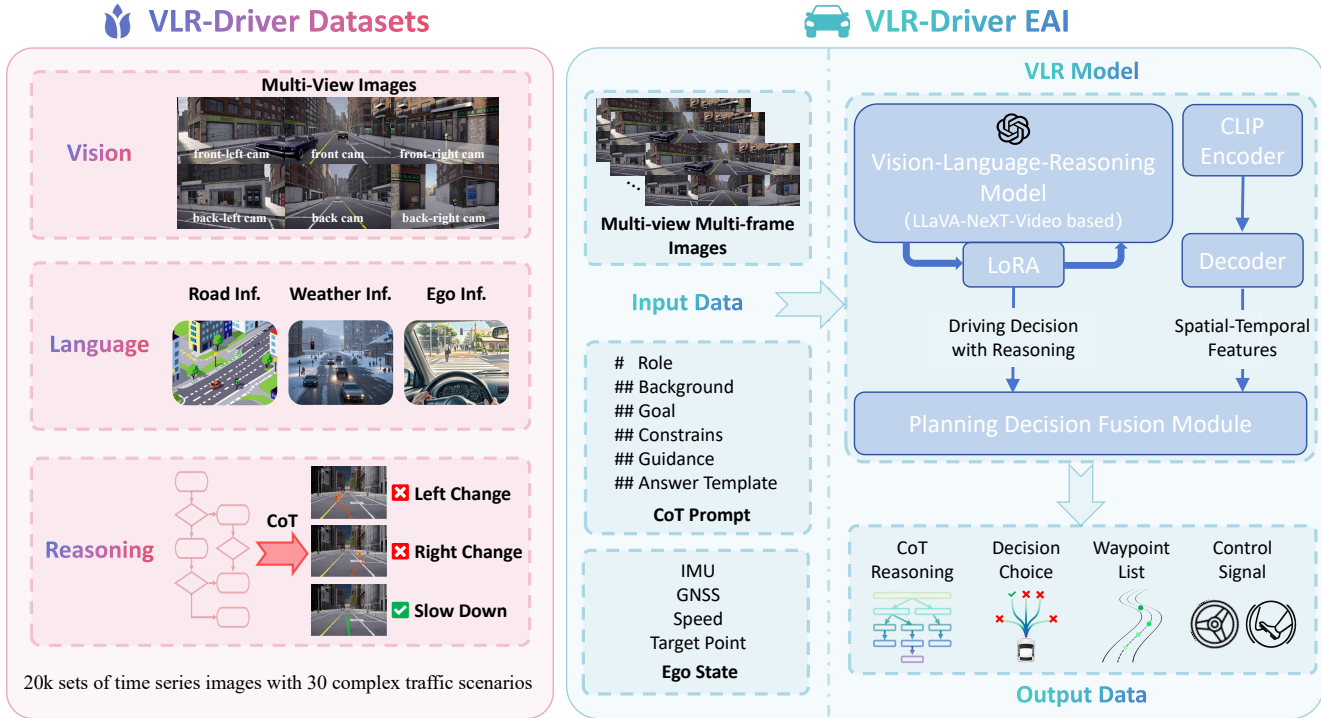


Figure 2. **Overview of VLR-Driver framework.** We introduce **VLR-Driver Dataset**, an advanced visual-language-reasoning dataset designed for autonomous driving, featuring detailed annotations of scene descriptions, analytical reasoning, and behavioral decisions. We present **VLR-Driver**, a novel multi-modal visual-language-reasoning framework for embodied autonomous driving that leverages a hierarchical spatiotemporal CoT reasoning mechanism.

tween sensor data can lead to inconsistencies, increasing both model complexity and training difficulty.

## 2.2. VLM and VLA in Autonomous Driving

VLMs unify visual perception with natural language processing capabilities, enabling a more comprehensive understanding of driving environments [19, 36, 37]. By incorporating cross-modal data fusion, integrating textual information alongside visual inputs, these systems gain text comprehension and human interaction capabilities that conventional E2E models inherently lack. DriveGPT4 [45] enhances LLMs' ability to process multimodal inputs by projecting them into the text domain, thereby enabling interpretable end-to-end autonomous driving. Senna [24] and DriveVLM [35] integrate VLMs with either traditional modular pipelines or E2E frameworks, achieving a decoupling between high-level planning and low-level trajectory prediction. This approach enhances planning performance while preserving the model's common sense reasoning capabilities.

Moreover, VLA represents an emerging paradigm that unifies visual perception, natural language understanding, and action prediction within a cohesive framework [13, 26]. Originally introduced in the field of robotics, RT-2 [4] pioneered the representation of robotic actions as text to-

kens, seamlessly incorporating them alongside natural language labels into the model's training set. This approach facilitates the direct transfer of internet-scale knowledge to robotic control, significantly enhancing both the generalization and semantic reasoning capabilities of robotic systems. In the context of autonomous driving, CoVLA [2] introduces an interpretable VLA model, seamlessly integrating visual perception, language-based scene understanding, and action planning. This integration enhances the system's ability to comprehend complex driving scenarios, anticipate trajectory outcomes, and execute informed driving decisions. However, despite these advancements, VLA models still exhibit limitations in accurately predicting precise control action values, leading to a low lower-bound in autonomous driving performance. Furthermore, when confronted with highly dynamic and complex traffic scenarios, their deep understanding and reasoning capabilities remain insufficient. Unlike the above methods, our proposed VLR model places greater emphasis on step-by-step reasoning and the thought process of the model, providing drivers with increased confidence in using autonomous driving systems.

## 2.3. Chain of Thought

The CoT technology is an extension of prompt engineering, proposed by Wei Jason in 2022 [40], which has greatly

154  
155  
156  
157  
158  
159  
160  
161  
162  
163  
164  
165  
166  
167  
168  
169  
170  
171  
172  
173  
174  
175  
176  
177  
178  
179  
180  
181  
182  
183  
184  
185  
186  
187  
188  
189  
190  
191  
192  
193  
194  
195  
196  
197  
198  
199  
200  
201

improved the effectiveness of reasoning for complex problems. The highly anticipated Deepseek-R1 [33] model also utilizes the CoT technique, which deeply integrates multi-modal knowledge base data, enabling the model to generate a step-by-step thinking process. DriveCoT [38] has built a CoT dataset that includes sensor data, control decisions, and CoT labels used to indicate reasoning processes. The model trained on this basis can generate predictions and final decisions with CoT, effectively improving model performance. LanguageMPC [30] combines LLM with Model Predictive Control and decomposes driving decisions into multiple subtasks through a CoT framework. This method enables the auto drive system to think like human beings, and improves its ability to handle complex scenes. Open-EMMA [44] introduces CoT technology to guide model generation of detailed descriptions of key objects, behavioral insights, and meta driving decisions, improving system transparency and usability. Motivated by these advancements, we apply step-by-step hierarchical spatiotemporal CoT to autonomous driving, enhancing the interpretability of reasoning and decision-making.

### 3. Method

We present the motivation and design details of our VLR-Driver framework. As depicted in Fig. 2, VLR-Driver comprises two main components: the VLR-Driver Embodied Agent and the VLR-Driver Dataset. Initially, we introduce the design concept of the VLR model, which builds upon enhancements to the VLA model (Sec. 3.1). Subsequently, we elaborate on the hierarchical spatiotemporal CoT methodology (Sec. 3.2) and the specifics of the dual-phase training strategy (Sec. 3.3).

#### 3.1. Overview

The VLR model is a large visual-language-reasoning model designed for embodied autonomous driving. It can processes visual inputs, such as multi-view images, alongside textual information, including vehicle control signals. The model is capable of extracting spatiotemporal key features within a multi-modal embedding and recursively analyzing potential safety risks and the driving intentions of other agents within the reasoning level of the VLR model. Ultimately, it formulates a comprehensive reasoning framework and well-structured decision-making outputs, explicitly identifying critical risk factors and the underlying rationale behind each decision. This process significantly reinforces the robustness and safety of the autonomous driving system, ensuring adaptive resilience in complex and dynamic environments.

In this study, we employ pre-trained LLaVA-NeXT-Video [50] as the VLM and CLIP [29] as the visual encoder. The model is capable of processing multi-frame multi-view image data that capture historical temporal context, while

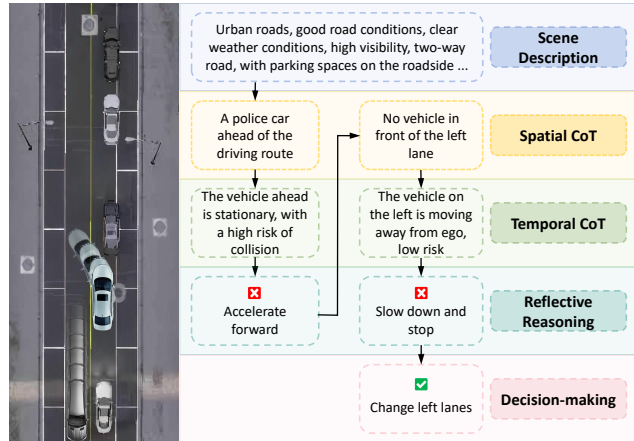


Figure 3. Illustration of the ST-CoT reasoning process. In this scenario, where some vehicles are illegally parked ahead and blocking the lane, our method can conduct hierarchical spatiotemporal reasoning analysis and make a decision of change left lane once the adjacent lane is free.

also extracting real-time vehicle sensor information to facilitate dynamic and context-aware decision-making.

**Input Representations.** We utilize  $N_f$  frame and  $N_v$  view images from the past period, with a field of view (FoV) of 70 degrees. It can be represented as  $V \in \mathbb{R}^{N_f \times N_v \times 3 \times H_0 \times W_0}$ . At the same time, there are also the current position  $(x, y)$  of ego vehicle, the speed  $v$ , the target point position  $(p, q)$ . Subsequently, the compressed and cropped image data and the information from the ego's sensors are input into the model.

**Output Representations.** Our output consists of the reasoning process and driving decisions generated by the VLR model for the current driving scenario. This includes risk identification, traffic signal recognition, motion direction prediction, and autonomous driving decision-making. The driving decision will also be fused with the spatiotemporal information features extracted by the E2E model, and finally output the waypoints and control signals of the vehicle for the next moment.

#### 3.2. Spatiotemporal CoT Reasoning

To enhance the reasoning capabilities and transparency of the autonomous driving system, we introduce a hierarchical ST-CoT that guides the model to approach driving decisions in a human-like manner. Our method decomposes the driving decision-making process into two levels: a perception-level spatiotemporal CoT  $C_{perception}$ , which focuses on extracting and understanding environmental dynamics, and a decision-level dynamic CoT  $C_{decision}$ , which refines and optimizes decision-making based on contextual and temporal factors. The example of CoT is shown in Fig. 3.

283 **3.2.1. Perception Level CoT**

284 The spatiotemporal characteristics of the environment play  
285 a crucial role in the autonomous driving process. The per-  
286 ception level CoT is responsible for guiding the model to  
287 extract spatial and temporal features from input image data,  
288 identify and locate crucial objects in the traffic, such as ve-  
289 hicles, pedestrians, alien objects, traffic lights, traffic signs,  
290 etc., and extract historical behavioral features of dynamic  
291 agent based on temporal information. Our method enables  
292 VLR model to describe the current driving scenario, con-  
293 struct real-time spatial layout and dynamic changes of the  
294 environment, and achieve long-term planning for driving  
295 decisions.

296 **Spatial CoT.** In driving scenarios, we primarily focus on  
297 obstacles that impact the ego’s normal operation, including  
298 object categories  $O_{type}$  and distances with the ego  $O_{dis}$ . A  
299 critical aspect of safe driving is identifying potential risk  
300 points within the current lane. Additionally, when the ve-  
301 hicle executes lane changes, objects in adjacent lanes, both  
302 left and right, may significantly influence its movement. Be-  
303 yond obstacles, key traffic light  $S_{light}$ , traffic signs  $S_{sign}$ ,  
304 and lane markings  $S_{mark}$  are also integral to decision-  
305 making, ensuring comprehensive spatial awareness.

306 **Temporal CoT.** While a single-frame image can provide  
307 a static representation of road scenes and traffic partici-  
308 pants, it fails to capture the motion trends of moving agents.  
309 To address this limitation, we introduce consecutive frames  
310  $I = \{I_f, I_{fr}, I_{fl}, I_b, I_{bl}, I_{br}\}_{t=T_{now}-T}^{T_{now}}$  into the model, al-  
311 lowing it to track temporal variations in object positioning,  
312 which  $I_f, I_{fr}, I_{fl}, I_b, I_{bl}, I_{br}$  represents the image view of  
313 front, front left, front right, back, back left and back right.  
314 These sequential frames not only offer instantaneous spa-  
315 tial context but also reveal motion trajectories and behav-  
316 ior patterns through their inter-frame positional changes.  
317 This temporal information is essential for predicting dy-  
318 namic object movement, assessing collision risks, and gen-  
319 erating robust path planning strategies, ultimately enhanc-  
320 ing the ability of anticipate and react to evolving traffic  
321 conditions.

322 **3.2.2. Decision Level CoT**

323 The output information from the perception-level serves as  
324 a critical foundation for the driving decision level, enabling  
325 reliable autonomous driving behavior inference. Within the  
326 driving decision level, we account for complex dynamic en-  
327 vironmental factors, transforming spatial and temporal in-  
328 formation from the perception level into concrete driving  
329 decisions. Specifically, decision-makers must not only an-  
330alyze the current driving environment in real time but also  
331 anticipate future behaviors of other traffic participants and  
332 make decisions based on multiple factors. Throughout this

process, the CoT in the driving decision level spans mul-  
333 tiple perspectives, incorporating safety, efficiency, comfort,  
334 and compliance with traffic regulations to ensure that driv-  
335 ing decisions meet safety standards while optimizing driv-  
336 ing efficiency.

To further enhance the structured reasoning process in  
337 autonomous driving, we have carefully designed hierarchi-  
338 cal reasoning prompts that guide decision-making. Our  
339 structured prompts follow a logical sequence of “risk point  
340 recognition — driving intention prediction — driving deci-  
341 sion selection”, forming a cohesive reasoning chain aligned  
342 with human cognitive driving patterns.

**Risk Point Recognition.** In this initial stage, the prompt-  
343 driven model conducts a comprehensive perception and  
344 analysis of the driving environment. This includes recog-  
345 nizing and evaluating critical elements such as traffic signs,  
346 lane markings, pedestrians, and obstacles to identify poten-  
347 tial risks.

**Driving Intention Prediction.** Once risk points are iden-  
351 tified, the model leverages dynamic target behavior predic-  
352 tion and scene understanding to infer the potential move-  
353 ments and intentions of other road users. For instance, the  
354 model assesses whether pedestrians are likely to cross the  
355 road or whether the vehicle ahead intends to change lanes.

**Driving Decision Selection.** Based on the contextual in-  
357 formation gathered from the first two stages, the model ap-  
358 plies multimodal information fusion and weighted decision-  
359 making to select the most optimal driving maneuver.

Through this structured prompting strategy, the large  
361 model adheres to a progressive reasoning hierarchy, begin-  
362 ning with fundamental environmental perception and ad-  
363 vancing to higher-level decision-making. By explicitly pre-  
364 senting the reasoning process in a clear and structured man-  
365 ner, this approach enhances passenger trust and confidence  
366 in the intelligent driving system. Moreover, the integration  
367 of recursive CoT reasoning enables the model to mimic the  
368 step-by-step thought process of human drivers, facilitating  
369 more flexible, reliable, and interpretable decision outputs in  
370 complex driving scenarios. The structured prompt frame-  
371 work are shown in Fig. 3.

372 **3.3. Training Paradigm**

VLR-Driver adopts a dual-phase training strategy to opti-  
374 mize its reasoning and decision-making capabilities. In the  
375 first phase, LoRA [16] is utilized for supervised fine-tuning  
376 on a pre-trained large model, enabling efficient adaptation  
377 with minimal memory and computational overhead while  
378 maintaining strong performance. In the second phase, Step-  
379 GRPO is applied for reinforcement learning based on hu-  
380 man preferences, further enhancing the model’s ability to  
381

382 exhibit human-like reasoning and decision-making characteristics.  
383

384 **Training with LoRA.** LoRA is a parameter-efficient fine-  
385 tuning technique that enables effective model adaptation by  
386 performing a low-rank decomposition of the weight matrix.  
387 The core principle behind LoRA is to decompose the weight  
388 matrix of a pre-trained model into a low-rank structure,  
389 significantly reducing the number of trainable parameters  
390 while preserving expressivity. Specifically, if the weight  
391 matrix in the pre-trained model is denoted as  $\mathbf{W}_0 \in \mathbb{R}^{d \times k}$ ,  
392 LoRA represents it as:

$$393 \quad \mathbf{W}' = \mathbf{W}_0 + \Delta \mathbf{W} = \mathbf{W}_0 + \frac{\alpha}{r} \mathbf{B} \cdot \mathbf{A}, \quad (1)$$

394 where  $\mathbf{A} \in \mathbb{R}^{r \times k}$  and  $\mathbf{B} \in \mathbb{R}^{d \times r}$ ,  $r$  is the rank of a low rank  
395 matrix, usually much smaller than  $d$  and  $k$ ,  $\alpha$  is a scaling  
396 factor. The forward pass is computed as:

$$397 \quad y = \mathbf{W}'x = \left( \mathbf{W}_0 + \frac{\alpha}{r} \mathbf{B} \cdot \mathbf{A} \right) x, \quad (2)$$

398 where  $y$  is the output and  $x$  is input.

399 We use LoRA for all linear modules, which not only  
400 saves computation but also ensures the performance of the  
401 model.

402 **Training with GRPO.** The core principle of GRPO [34]  
403 is to optimize strategies by assigning relative rewards to  
404 multiple outputs generated from the same prompt, thereby  
405 eliminating the need for additional value function models.  
406 The introduction of process reward model estimation in  
407 GRPO provides finer support for distributed rewards. The  
408 reward of each step of the outputs is:

$$409 \quad R = \left\{ \left\{ r_1^{index(1)} ; \dots ; r_1^{index(K_1)} \right\} ; \dots ; \left\{ r_G^{index(1)} ; \dots ; r_G^{index(K_G)} \right\} \right\}, \quad (3)$$

410 where  $index(\cdot)$  is the end token index, and the reward need  
411 be normalized as:

$$412 \quad \tilde{r}_i^{index(j)} = \frac{r_i^{index(j)} - \text{mean}(R)}{\text{std}(R)}. \quad (4)$$

413 We extend GRPO by introducing reasoning Step-GRPO,  
414 a supervised reasoning decision process that structures the  
415 output into multiple steps based on the CoT reasoning  
416 framework. At each step, a reward function is applied to  
417 evaluate and assign scores, enabling fine-grained feedback  
418 that enhances model interpretability and accelerates con-  
419 vergence. Specifically, we first generate multiple candi-  
420 date decision answers for the current driving scenario us-  
421 ing prompts within the VLR model; Then, following our  
422 ST-CoT strategy, the reasoning process is divided into four  
423 distinct steps: scene description, spatial risk point reason-  
424 ing, dynamic trajectory prediction, and driving decision-  
425 making; Furthermore, each reasoning step is assigned a re-  
426 ward to encourage structured learning. Finally, we compare

427 all answers within the group and calculate the Kullback-  
428 Leibler (KL) divergence to update the policy model. This  
429 grouping and step-by-step scoring strategy enhances train-  
430 ing efficiency and reduces the likelihood of erroneous rea-  
431 soning in the model.

## 4. VLR-Driver Dataset

432 To fully explore the reasoning and decision-making capabili-  
433 ties of large language models, we propose an advanced rea-  
434 soning and decision-making dataset for autonomous driv-  
435 ing scenarios, called the VLR-Driver Datasets. This dataset  
436 relies on the CARLA [14] simulator for data collection  
437 and is expanded and meticulously annotated based on the  
438 Bench2Drive dataset [22]. It includes: a) multi-view multi-  
439 frame images or videos, b) valuable information for au-  
440 tonomous driving, such as road details, weather conditions,  
441 vehicle information, and scene descriptions, and c) driv-  
442 ing decision choices along with the decision-making pro-  
443 cess based on a ST-CoT. This dataset provides a rich and  
444 comprehensive training foundation for autonomous driving  
445 reasoning and decision-making, allowing the agent to ex-  
446 hibit human-like reasoning while interacting with the envi-  
447 ronment. The dataset includes 20,000 sets of multi-frame,  
448 multi-angle image data collected from various road con-  
449 ditions such as urban, rural, and highways in the CARLA  
450 simulator, covering over 40 specific complex traffic scenar-  
451 os (e.g., forward accidents, dynamic object crossings, etc.).  
452 Each image set provides road scene descriptions, environ-  
453 mental weather information, vehicle status data, and, most  
454 importantly, the human-like reasoning process and driving  
455 behavior decisions.

### 4.1. Data Collection

457 We conducted data collection based on the 44 corner scene  
458 classifications provided by Bench2Drive to ensure optimal  
459 autonomous driving performance in various complex corner  
460 scenarios. The Bench2Drive dataset offers a rich array of  
461 data and annotations, including multi-angle images, lidar,  
462 radar, vehicle information, and expert assessments, which  
463 have been instrumental in building our VLR dataset. Ad-  
464 ditionally, we selected over 40 scenes where autonomous  
465 driving's reasoning and decision-making capabilities are  
466 relatively weak, using them as the visual and textual com-  
467 ponents of our dataset. We further expanded and enriched the  
468 dataset by collecting additional data in the CARLA simula-  
469 tor. We have taken into account various weather conditions,  
470 road conditions, and the types and numbers of traffic partic-  
471 ipants in the scene.

472 **Weather.** For each scene, we randomly set values  
473 for cloudiness, fog density, precipitation, precipitation de-  
474 posits, sun altitude angle, sun azimuth angle, wetness, and  
475 wind intensity. The combinations of these parameters cover  
476 a variety of weather conditions, such as sunny, rainy, foggy,

Table 1. The comparison of core metrics and subdivision infraction scores with state-of-the-art E2E/VLM models on the Bench2Drive benchmark. C, L and T indicate camera, LiDAR and text modalities, respectively. DS, RC, IS, SR correspond to the Driving Score, Route Completion, Infraction Score, and Success Rate. CP, CV, CL, RL, SS, OR, AB, YEV correspond to the Collision with a Pedestrian, Collision with another Vehicle, Collision with Layout, Red Light infractions, Stop Sign infractions, Off-Road infractions, Agent Blocked, and failure to Yield to Emergency Vehicles infractions.

Method	Type	Modality	Core Metrics ↑				Subdivision Infraction Score ↓							
			DS	RC	IS	SR	CP	CV	CL	RL	SS	OR	AB	YEV
NEAT [10]	E2E	C	30.86	55.35	0.55	6.81	1.08	9.87	5.57	0.20	1.33	0.41	2.01	0.27
TCP [42]		C	56.28	83.57	0.65	25.00	<b>0.26</b>	5.46	5.46	<b>0.00</b>	0.52	0.22	0.78	<b>0.00</b>
LeTFuser [1]		C+L	52.53	77.68	0.67	18.18	1.16	5.54	3.79	0.29	0.87	0.12	0.58	0.29
LateFusion [28]		C+L	48.53	58.32	0.85	18.18	0.38	3.11	1.55	0.38	0.77	0.06	1.55	0.38
TransFuser [11]		C+L	37.18	68.14	0.51	9.09	0.96	13.24	8.71	<b>0.00</b>	0.96	0.32	2.58	0.32
ThinkTwice [21]		C+L	58.79	74.35	0.77	29.54	0.30	5.76	0.91	<b>0.00</b>	0.91	0.05	0.91	0.30
EATNet [9]		C+L	42.97	78.84	0.54	15.91	0.82	14.01	1.92	<b>0.00</b>	1.64	0.22	1.09	0.27
InterFuser [31]		C+L	63.81	80.46	0.79	40.90	0.35	3.81	0.54	0.27	1.08	0.05	0.54	0.27
LMDrive [32]	VLM	C+L+T	24.76	33.02	<b>0.90</b>	13.63	1.14	2.86	2.29	<b>0.00</b>	0.57	0.05	3.44	0.57
LeapAD [27]		C+T	55.18	77.45	0.71	36.36	0.69	5.07	1.15	0.20	0.91	0.08	1.47	0.27
VLR-Driver (Ours)	VLR	C+T	<b>75.00</b>	<b>86.08</b>	0.87	<b>50.00</b>	0.72	<b>2.83</b>	<b>0.48</b>	<b>0.00</b>	<b>0.48</b>	<b>0.04</b>	<b>0.24</b>	0.24

Table 2. The comparison of driving advanced ability and experience score with state-of-the-art models on the Bench2Drive benchmark. OT, MER, EB, GW, TS, DE, SC correspond to the OverTak-ing, MERging, Emergency Brake, Give Way, Traffic Sign, Driving Efficiency, and Smoothness Control.

Method	Driving Advanced Ability ↑						Exper. Score ↑	
	OT	MER	EB	GW	TS	Mean	DE	SC
NEAT [10]	0.00	6.66	9.09	<b>50.00</b>	27.77	18.70	92.09	0.30
TCP [42]	25.00	13.33	27.27	<b>50.00</b>	50.00	33.12	114.52	0.27
LeTFuser [1]	0.00	20.00	18.18	0.00	47.22	17.08	115.09	0.47
LateFusion [28]	0.00	20.00	9.09	0.00	36.11	13.04	104.39	<b>0.59</b>
TransFuser [11]	0.00	13.33	9.09	0.00	36.11	11.71	95.20	0.36
ThinkTwice [21]	12.50	20.00	36.36	<b>50.00</b>	52.77	34.33	91.17	0.36
EATNet [9]	0.00	13.33	18.18	0.00	41.66	14.63	88.13	0.33
InterFuser [31]	0.00	46.66	54.54	<b>50.00</b>	61.11	42.46	119.20	0.32
LMDrive [32]	25.00	6.66	9.09	<b>50.00</b>	2.77	18.70	75.41	0.22
LeapAD [27]	12.50	33.33	27.27	<b>50.00</b>	44.44	33.51	93.33	0.26
VLR-Driver (Ours)	<b>37.50</b>	<b>46.66</b>	<b>72.72</b>	<b>50.00</b>	<b>72.22</b>	<b>55.82</b>	<b>125.22</b>	<b>0.59</b>

broken sky, and stormy, as well as different lighting conditions for day and night.

**Roads.** The scenes include various road types such as urban two-way single-lane roads, multi-lane roads, highways, and narrow rural roads.

**Traffic Participants.** Different corner cases involve various traffic participants, including cars, bicycles, pedestrians, ambulances, etc., simulating the complex traffic conditions encountered in daily driving.

## 4.2. Data Annotation

The reasoning chain process and the decision-making choices are crucial for training large autonomous driving models and are key to enhancing the model’s human-like reasoning ability. Therefore, we performed secondary annotation on the dataset we collected.

**Driving Scene Descriptions.** We used the pre-trained large visual language model Qwen2-VL [3] to generate detailed descriptions for the corresponding driving scenes. These descriptions primarily focus on environmental infor-

mation such as road conditions, weather, and lighting, as well as dynamic targets like vehicles and pedestrians that may pose driving risks.

**Reasoning Decisions and Process.** We considered pre-annotated information such as vehicle speed, acceleration, steering angle, traffic light status, and the state of the vehicle ahead. A rule-based method was used to determine the true values of future motion behaviors based on the decision choices made at earlier time steps. Additionally, we completed the predefined CoT reasoning text statements. Finally, to ensure the accuracy and consistency of the annotations, especially for decision choices, carefully manual verification was carried out.

## 5. Experiment

### 5.1. Experimental Setup

Our method was validated on the open source autonomous driving simulation platform CARLA 0.9.15 [14]. The VLR-Driver model was trained on a server equipped with 8 NVIDIA A800 GPUs (each with 80G of video memory) for approximately 50 hours. The dataset used was the VLR-Driver dataset that we developed. Specifically, we use ViT-g/14 from EVA-CLIP [29] as the vision encoder and LLaVA-NeXT-Video-7B [50] as the VLM. The resolution of the input image is set to  $336 \times 336$  pixels.

### 5.2. Metrics

We employ four core metrics to evaluate autonomous driving performance: driving score (DS), route completion (RC), infraction score (IS), and success rate (SR). Additionally, to provide a more granular assessment of model performance in specific aspects, we introduce three supplementary evaluation categories: subdivision infraction score, driving advanced ability, and driving experience score [22].

Table 3. Ablation study for each module.

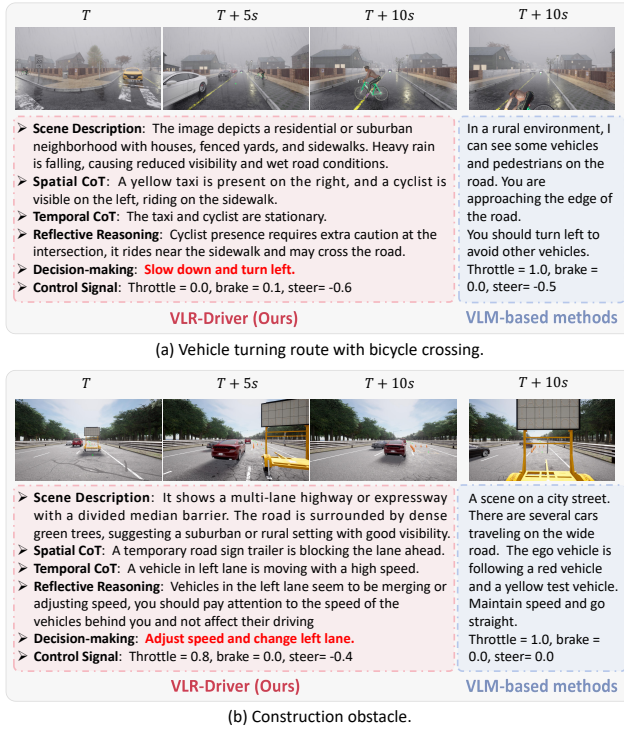


Figure 4. Visual comparison between VLR-Driver and VLM-based methods. The ST-CoT guides the VLR model to approach driving decisions in a human-like spatiotemporal manner. Based on the sequence of images from the preceding time period  $T$ , we derive the following inference results. The images captured at 5 and 10 seconds afterward validate the accuracy of our decisions.

529

### 5.3. Comparisons with Existing Methods

We conducted comprehensive experiments with the SOTA methods including E2E and VLM in the CARLA simulator with Bench2Drive Benchmark. We present comparison result in Tab. 1. It can be seen that our method outperforms other methods in key metrics such as DS, RC, and SR, achieving first place and effectively improving DS by 17.5%, mean of driving ability by 31.4%, and SR by 22.2%.

The comparison results of the driving advanced ability and driving experience score of each method are shown in Tab. 2. Our method achieved the best results in all abilities, thanks to the deep reflection and reasoning ability of our VLR model, which has stronger traffic reasoning capacity in special road conditions. Most E2E methods can only achieve following the vehicle, but when there is a vehicle temporarily parked in the lane ahead, blocking the self driving route, they will keep stopping and waiting, making it impossible to complete the entire route. And our VLR-Driver can achieve deep understanding and inference of the current scene through large-scale model inference, so as to make timely detours.

ID	Abal.	Exp.	Core Metrics ↑		Driving Advanced Ability ↑		
			DS	SR	OT	MER	EB
1	VLR	Full Model	<b>71.48</b>	<b>54.54</b>	<b>37.50</b>	<b>46.66</b>	<b>72.72</b>
2		w/o CoT	57.17	34.09	25.00	40.00	41.66
3	Arch.	w/o VLR-Model	46.39	20.45	14.28	26.66	36.36
4		w/o VLR-Data	52.85	27.27	25.00	26.66	9.09
5	Train	w/o Step-GRPO	65.57	45.45	37.50	40.00	63.63

## 5.4. Ablation Study

We conducted a comprehensive ablation study, detailed in Tab. 3. The experimental configurations include four variants: (1) Without utilizing our proposed spatiotemporal CoT strategy, using only a question-based approach without reasoning guidance. (2) Without using our VLR model, instead employing a standard LLM module. (3) Removing the VLR data used to guide the reasoning process. (4) Without Step-GRPO reinforcement learning training, using only LoRA strategies to fine-tune the model with supervision. The results show the effectiveness of each contribution.

## 5.5. Visualization

We selected some special scenarios to visualize the performance in complex traffic situations with reflective reasoning, and the comparison results shown in Fig. 4. The ST-CoT enables the model to make driving decisions with human-like reasoning, considering both spatial and temporal dynamics. More visual comparison results can be found in the Appendix.

## 6. Conclusion

In this paper, we introduce VLR-Driver, a VLR model for embodied AD. It leverages a carefully designed ST-CoT strategy to guide the model in recursively analyzing potential safety risks and the driving intentions of dynamic agents in complex traffic scenarios. Our dual-phase training method significantly enhances the generalization of the model. Additionally, we propose the VLR-Driver dataset, which effectively integrates spatiotemporal perception, language understanding, and reflective reasoning, providing crucial support for interpretability reasoning in AD system. Experimental results show that VLR-Driver outperforms other methods on Bench2Drive, achieving cutting-edge performance and paving the way for EAI realization.

**Limitations and future work.** There are differences between the data in simulation platforms and the real world. How to transfer and adapt it to a real-world style remains an important area for further exploration.

587 **References**

- 588 [1] Pedram Agand, Mohammad Mahdavian, Manolis Savva, and  
589 Mo Chen. Lefuser: Light-weight end-to-end transformer-  
590 based sensor fusion for autonomous driving with multi-task  
591 learning. 2023. 2, 7
- 592 [2] Hidehisa Arai, Keita Miwa, Kento Sasaki, Yu Yamaguchi,  
593 Kohei Watanabe, Shunsuke Aoki, and Issei Yamamoto.  
594 Covla: Comprehensive vision-language-action dataset for  
595 autonomous driving. *ArXiv*, abs/2408.10845, 2024. 1, 3
- 596 [3] Jinze Bai, Shuai Bai, Yunfei Chu, Zeyu Cui, Kai Dang,  
597 Xiaodong Deng, Yang Fan, Wenbin Ge, Yu Han, Fei  
598 Huang, et al. Qwen technical report. *arXiv preprint*  
599 *arXiv:2309.16609*, 2023. 7
- 600 [4] Anthony Brohan, Noah Brown, Justice Carbajal, Yevgen  
601 Chebotar, Xi Chen, Krzysztof Choromanski, Tianli Ding,  
602 Danny Driess, Avinava Dubey, Chelsea Finn, Pete Florence,  
603 Chuyuan Fu, Montse Gonzalez Arenas, Keerthana Gopalakrishnan,  
604 Kehang Han, Karol Hausman, Alexander Herzog,  
605 Jasmine Hsu, Brian Ichter, Alex Irpan, Nikhil Joshi, Ryan  
606 Julian, Dmitry Kalashnikov, Yuheng Kuang, Isabel Leal,  
607 Lisa Lee, Tsang-Wei Edward Lee, Sergey Levine, Yao Lu,  
608 Henryk Michalewski, Igor Mordatch, Karl Pertsch, Kanishka  
609 Rao, Krista Reymann, Michael Ryoo, Grecia Salazar,  
610 Pannag Sanketi, Pierre Sermanet, Jaspiar Singh, Anikait  
611 Singh, Radu Soricu, Huong Tran, Vincent Vanhoucke, Quan  
612 Vuong, Ayzaan Wahid, Stefan Welker, Paul Wohlhart, Jialin  
613 Wu, Fei Xia, Ted Xiao, Peng Xu, Sichun Xu, Tianhe Yu,  
614 and Brianna Zitkovich. Rt-2: Vision-language-action models  
615 transfer web knowledge to robotic control. 2023. 3
- 616 [5] Daoming Chen, Ning Wang, Feng Chen, and Tony Pipe. De-  
617 trive: Imitation learning with transformer detection for end-  
618 to-end autonomous driving. 2023. 2
- 619 [6] Jianyu Chen, Zhuo Xu, and Masayoshi Tomizuka. End-  
620 to-end autonomous driving perception with sequential latent  
621 representation learning. 2020. 1
- 622 [7] Li Chen, Penghao Wu, Kashyap Chitta, Bernhard Jaeger, Andreas  
623 Geiger, and Hongyang Li. End-to-end autonomous  
624 driving: Challenges and frontiers. 2023. 1
- 625 [8] Shaoyu Chen, Bo Jiang, Hao Gao, Bencheng Liao, Qing  
626 Xu, Qian Zhang, Chang Huang, Wenyu Liu, and Xinggang  
627 Wang. Vadv2: End-to-end vectorized autonomous driving  
628 via probabilistic planning. 2024. 2
- 629 [9] Weihuang Chen, Fanjie Kong, Liming Chen, Shen'ao Wang,  
630 Zhiping Wang, and Hongbin Sun. Eatnet: Efficient axial  
631 transformer network for end-to-end autonomous driving. In  
632 *ITSC*, 2024. 7
- 633 [10] Kashyap Chitta, Aditya Prakash, and Andreas Geiger. *NEAT:*  
634 *Neural Attention Fields for End-to-End Autonomous Driving*.  
635 2021. 2, 7
- 636 [11] Kashyap Chitta, Aditya Prakash, Bernhard Jaeger, Zehao Yu,  
637 Katrin Renz, and Andreas Geiger. Transfuser: Imitation  
638 with transformer-based sensor fusion for autonomous driving.  
639 *PAMI*, Vol.45(No.11):12878–12895, 2023. 2, 7
- 640 [12] Can Cui, Yunsheng Ma, Xu Cao, Wenqian Ye, Yang Zhou,  
641 Kaizhao Liang, Jintai Chen, Juanwu Lu, Zichong Yang,  
642 Kuei-Da Liao, Tianren Gao, Erlong Li, Kun Tang, Zhipeng  
643 Cao, Tong Zhou, Ao Liu, Xinrui Yan, Shuqi Mei, Jianguo  
Cao, Ziran Wang, and Chao Zheng. A survey on multimodal  
large language models for autonomous driving. 2023. 1 644
- [13] Pengxiang Ding, Han Zhao, Zhitao Wang, Zhenyu Wei,  
Shangke Lyu, and Donglin Wang. Quar-vla: Vision-  
language-action model for quadruped robots. 2023. 3 645
- [14] Alexey Dosovitskiy, German Ros, Felipe Codella, Antonio  
Lopez, and Vladlen Koltun. Carla: An open urban driving  
simulator. In *CoRL*, pages 1–16. PMLR, 2017. 6, 7 646
- [15] Hao Gao, Shaoyu Chen, Bo Jiang, Bencheng Liao, Yang  
Shi, Xiaoyang Guo, Yuechuan Pu, Haoran Yin, Xiangyu Li,  
Xinbang Zhang, Ying Zhang, Wenyu Liu, Qian Zhang, and  
Xinggang Wang. Rad: Training an end-to-end driving policy  
via large-scale 3dgs-based reinforcement learning. 2 647
- [16] Edward J Hu, Yelong Shen, Phillip Wallis, Zeyuan Allen-  
Zhu, Yuanzhi Li, Shean Wang, Lu Wang, Weizhu Chen, et al.  
Lora: Low-rank adaptation of large language models. *ICLR*,  
1(2):3, 2022. 2, 5 648
- [17] Shengchao Hu, Li Chen, Penghao Wu, Hongyang Li, Junchi  
Yan, and Dacheng Tao. *ST-P3: End-to-End Vision-Based Au-  
tonomous Driving via Spatial-Temporal Feature Learning*.  
2022. 2 649
- [18] Zhiyu Huang, Haochen Liu, and Chen Lv. Gameformer:  
Game-theoretic modeling and learning of transformer-based  
interactive prediction and planning for autonomous driving.  
In *ICCV*, pages 3903–3913. 1 650
- [19] Jyh-Jing Hwang, Runsheng Xu, Hubert Lin, Wei-Chih Hung,  
Jingwei Ji, Kristy Choi, Di Huang, Tong He, Paul Covington,  
and Benjamin Sapp. Emma: End-to-end multimodal model  
for autonomous driving. *arXiv preprint arXiv:2410.23262*,  
2024. 3 651
- [20] Xiaosong Jia, Yulu Gao, Li Chen, Junchi Yan, Patrick  
Langchuan Liu, and Hongyang Li. Driveadapter:  
Breaking the coupling barrier of perception and planning in  
end-to-end autonomous driving. In *ICCV*, pages 7953–7963.  
2 652
- [21] Xiaosong Jia, Penghao Wu, Li Chen, Jiangwei Xie, Cong-  
gui He, Junchi Yan, and Hongyang Li. *Think Twice be-  
fore Driving: Towards Scalable Decoders for End-to-End  
Autonomous Driving*. 2023. 2, 7 653
- [22] Xiaosong Jia, Zhenjie Yang, Qifeng Li, Zhiyuan Zhang, and  
Junchi Yan. Bench2drive: Towards multi-ability benchmark-  
ing of closed-loop end-to-end autonomous driving. *arXiv  
preprint arXiv:2406.03877*, 2024. 6, 7 654
- [23] Xiaosong Jia, Junqi You, Zhiyuan Zhang, and Junchi Yan.  
Drivetransformer: Unified transformer for scalable end-to-  
end autonomous driving. In *ICLR*, 2025. 2 655
- [24] Bo Jiang, Shaoyu Chen, Bencheng Liao, Xingyu Zhang, Wei  
Yin, Qian Zhang, Chang Huang, Wenyu Liu, and Xinggang  
Wang. Senna: Bridging large vision-language models and  
end-to-end autonomous driving. . 3 656
- [25] Bo Jiang, Shaoyu Chen, Qing Xu, Bencheng Liao, Jiajie  
Chen, Helong Zhou, Qian Zhang, Wenyu Liu, Chang Huang,  
and Xinggang Wang. Vad: Vectorized scene representation  
for efficient autonomous driving. In *ICCV*, pages 8340–  
8350, . 2 657
- [26] Yueen Ma, Zixing Song, Yuzheng Zhuang, Jianye Hao, and  
Irwin King. A survey on vision-language-action models for  
embodied ai. *ArXiv*, abs/2405.14093, 2024. 1, 3 658

- 702 [27] Jianbiao Mei, Yukai Ma, Xuemeng Yang, Licheng Wen,  
703 Xinyu Cai, Xin Li, Daocheng Fu, Bo Zhang, Pinlong Cai,  
704 and Min Dou. Continuously learning, adapting, and improv-  
705 ing: A dual-process approach to autonomous driving. *arXiv*  
706 preprint arXiv:2405.15324, 2024. 7
- 707 [28] Aditya Prakash, Kashyap Chitta, and Andreas Geiger. *Multi-*  
708 *Modal Fusion Transformer for End-to-End Autonomous*  
709 *Driving*. 2021. 7
- 710 [29] Alec Radford, Jong Wook Kim, Chris Hallacy, Aditya  
711 Ramesh, Gabriel Goh, Sandhini Agarwal, Girish Sastry,  
712 Amanda Askell, Pamela Mishkin, Jack Clark, et al. Learning  
713 transferable visual models from natural language super-  
714 vision. In *ICML*, pages 8748–8763. PMLR, 2021. 4, 7
- 715 [30] Hao Sha, Yao Mu, Yuxuan Jiang, Li Chen, Chenfeng Xu,  
716 Ping Luo, Shengbo Eben Li, Masayoshi Tomizuka, Wei  
717 Zhan, and Mingyu Ding. Languagempc: Large language  
718 models as decision makers for autonomous driving. *arXiv*  
719 preprint arXiv:2310.03026, 2023. 4
- 720 [31] Hao Shao, Letian Wang, Ruobing Chen, Hongsheng Li, and  
721 Yu Liu. Safety-enhanced autonomous driving using inter-  
722 pretative sensor fusion transformer. 2022. 7
- 723 [32] Hao Shao, Yuxuan Hu, Letian Wang, Steven L. Waslander,  
724 Yu Liu, and Hongsheng Li. Lmdrive: Closed-loop end-to-  
725 end driving with large language models. *CVPR*, 2024. 7
- 726 [33] Zhihong Shao, Peiyi Wang, Qihao Zhu, Runxin Xu, Junxiao  
727 Song, Xiao Bi, Haowei Zhang, Mingchuan Zhang, YK Li,  
728 Y Wu, et al. Deepseekmath: Pushing the limits of mathe-  
729 matical reasoning in open language models. *arXiv preprint*  
730 arXiv:2402.03300, 2024. 4
- 731 [34] Zhihong Shao, Peiyi Wang, Qihao Zhu, Runxin Xu, Junxiao  
732 Song, Xiao Bi, Haowei Zhang, Mingchuan Zhang, YK Li,  
733 Y Wu, et al. Deepseekmath: Pushing the limits of mathe-  
734 matical reasoning in open language models. *arXiv preprint*  
735 arXiv:2402.03300, 2024. 2, 6
- 736 [35] Xiaoyu Tian, Junru Gu, Bailin Li, Yicheng Liu, Chenxu Hu,  
737 Yang Wang, Kun Zhan, Peng Jia, Xianpeng Lang, and Hang  
738 Zhao. Drivevlm: The convergence of autonomous driving  
739 and large vision-language models. 2024. 1, 3
- 740 [36] Junming Wang, Xingyu Zhang, Zebin Xing, Songen Gu,  
741 Xiaoyang Guo, Yang Hu, Ziying Song, Qian Zhang, Xi-  
742 aoxiao Long, and Wei Yin. He-drive: Human-like end-to-  
743 end driving with vision language models. *arXiv preprint*  
744 arXiv:2410.05051, 2024. 3
- 745 [37] Shihao Wang, Zhiding Yu, Xiaohui Jiang, Shiyi Lan, Min  
746 Shi, Nadine Chang, Jan Kautz, Ying Li, and Jose M. Alvarez.  
747 Omnidrive: A holistic llm-agent framework for autonomous  
748 driving with 3d perception, reasoning and planning. 2024. 3
- 749 [38] Tianqi Wang, Enze Xie, Ruihang Chu, Zhenguo Li, and Ping  
750 Luo. Drivecot: Integrating chain-of-thought reasoning with  
751 end-to-end driving. *ArXiv*, abs/2403.16996, 2024. 2, 4
- 752 [39] Wenhui Wang, Jiangwei Xie, ChuanYang Hu, Haoming Zou,  
753 Jianan Fan, Wenwen Tong, Yang Wen, Silei Wu, Hanming  
754 Deng, Zhiqi Li, Hao Tian, Lewei Lu, Xizhou Zhu, Xiaogang  
755 Wang, Yu Qiao, and Jifeng Dai. Drivelmlm: Aligning multi-  
756 modal large language models with behavioral planning states  
757 for autonomous driving. 2023. 2
- 758 [40] Jason Wei, Xuezhi Wang, Dale Schuurmans, Maarten  
759 Bosma, Fei Xia, Ed Chi, Quoc V Le, Denny Zhou, et al.
- Chain-of-thought prompting elicits reasoning in large lan-  
guage models. In *NeurIPS*, pages 24824–24837, 2022. 2,  
3
- [41] Jiayang Wu, Wensheng Gan, Zefeng Chen, Shicheng Wan,  
and Philip S. Yu. Multimodal large language models: A sur-  
vey. 2023. 1
- [42] Penghao Wu, Xiaosong Jia, Li Chen, Junchi Yan, Hongyang  
Li, and Yu Qiao. Trajectory-guided control prediction for  
end-to-end autonomous driving: A simple yet strong base-  
line. 2022. 2, 7
- [43] Weishang Wu, Xiaoheng Deng, Ping Jiang, Shaohua Wan,  
and Yuanxiong Guo. Crossfuser: Multi-modal feature fusion  
for end-to-end autonomous driving under unseen weather  
conditions. *ITSC*, Vol.24(No.12):1–15, 2023. 2
- [44] Shuo Xing, Chengyuan Qian, Yuping Wang, Hongyuan Hua,  
Kexin Tian, Yang Zhou, and Zhengzhong Tu. Opennemma:  
Open-source multimodal model for end-to-end autonomous  
driving. *ArXiv*, abs/2412.15208, 2024. 4
- [45] Zhenhua Xu, Yujia Zhang, Enze Xie, Zhen Zhao, Yong Guo,  
Kenneth K.Y. Wong, Zhenguo Li, and Hengshuang Zhao.  
Drivegpt4: Interpretable end-to-end autonomous driving via  
large language model. 2023. 3
- [46] Zhenjie Yang, Xiaosong Jia, Hongyang Li, and Junchi Yan.  
Llm4drive: A survey of large language models for au-  
tonomous driving. 2023. 2
- [47] Tengju Ye, Wei Jing, Chunyong Hu, Shikun Huang, Ling-  
ping Gao, Fangzhen Li, Jingke Wang, Ke Guo, Wencong  
Xiao, Weibo Mao, Hang Zheng, Kun Li, Junbo Chen, and  
Kaicheng Yu. Fusionad: Multi-modality fusion for predic-  
tion and planning tasks of autonomous driving. 2023. 2
- [48] Shukang Yin, Chaoyou Fu, Sirui Zhao, Ke Li, Xing Sun,  
Tong Xu, and Enhong Chen. A survey on multimodal large  
language models. 2023. 1
- [49] Jiakai Zhang. *End-to-end Learning for Autonomous Driving*.  
Thesis, 2019. 1
- [50] Yuanhan Zhang, Bo Li, haotian Liu, Yong jae Lee, Liangke  
Gu, Di Fu, Jiashi Feng, Ziwei Liu, and Chunyuan Li. Llava-  
next: A strong zero-shot video understanding model, 2024.  
4, 7
- [51] Zhejun Zhang, Alexander Liniger, Dengxin Dai, Fisher Yu,  
and Luc Van Gool. End-to-end urban driving by imitating a  
reinforcement learning coach. 2021. 2
- [52] Rui Zhao, Qirui Yuan, Jinyu Li, Haofeng Hu, Yun Li,  
Chengyuan Zheng, and Fei Gao. Sce2drivex: A generalized  
mllm framework for scene-to-drive learning. *arXiv preprint*  
arXiv:2502.14917, 2025. 2
- [53] Z. Zhao, Q. Wu, J. Wang, B. Zhang, C. Zhong, and A. A.  
Zhilenkov. Exploring embodied intelligence in soft robotics:  
A review. *Biomimetics (Basel)*, 9(4), 2024. 1
- [54] Xingcheng Zhou, Mingyu Liu, Ekim Yurtsever, Bare Luka  
Zagar, Walter Zimmer, Hu Cao, and Alois C. Knoll. Vision  
language models in autonomous driving: A survey and out-  
look. *TIV*, pages 1–20, 2024. 2
- [55] Yunsong Zhou, Linyan Huang, Qingwen Bu, Jia Zeng,  
Tianyu Li, Hang Qiu, Hongzi Zhu, Minyi Guo, Yu Qiao, and  
Hongyang Li. Embodied understanding of driving scenarios.  
2024. 1